# SIMULATION OF UPWELLING THERMAL RADIATION SCATTERED BY AEROSOL ALLOWING FOR SURFACE TEMPERATURE INHOMOGENEITIES. I. POINT SPREAD FUNCTION

**S.V. Afonin, V.V. Belov, and I.Yu. Makushkina**

*Institute of Atmospheric Optics,*
*Siberian Branch of the Russian Academy of Sciences, Tomsk*
*Received December 30, 1994*

*Results of simulation of the point spread function (PSF) within the IR spectral range have been analyzed for different viewing geometry. The PSF has been examined as a function of the distance from an observation point, azimuth and zenith observation angles, and aerosol content in the ground layer of the atmosphere and the stratosphere.*

## 1. INTRODUCTION

Earlier in Refs. 1–3 we studied some patterns of formation of upwelling thermal radiation scattered by aerosol within the 3–5 and 8–13 μm spectral ranges. Contributions from single and multiple scattering as well as from the adjacency effect to the intensity of scattered radiation were estimated, and the dependence of the intensity on the optical aerosol and atmospheric meteorological parameters was determined.

Analysis of the characteristics of the adjacency effect caused by scattering of thermal radiation from regions of the Earth's surface external to the field of view of a receiving system in the direction toward a receiving device allows a conclusion about possible noticeable effect of the surface temperature inhomogeneities on the accuracy of correction (more than 0.5–1.0°) of satellite measurements of the underlying surface temperature for the contribution of a turbid atmosphere to be made. This result has motivated extension of investigations aimed at determination of relations of the parameters of the temperature surface inhomogeneities with the intensity of thermal radiation scattered by aerosol.

The paper presents results of calculations of the point spread function (PSF) which is the most convenient instrument for studying this problem on the basis of imitation simulation. Unfortunately, as we are well aware, the amount of data about the PSF, necessary for such studies in the IR spectral range, is lacking in the literature.

In this paper, results of calculations describing the spatial–angular PSF structure are presented in detail for various optical-geometric situations.

## 2. BASIC CHARACTERISTICS OF SIMULATION

The following characteristics are results of simulation: the intensity $J_\lambda$ and radiative temperature $T_\lambda$ of radiation emitted by the atmosphere–underlying surface (A–US) system

$$J_\lambda = J_\lambda^0 + J_\lambda^{MC}, \quad T_\lambda = B_\lambda^{-1}\,[J_\lambda],$$

$$J_\lambda^0 = J_{ATM}^0 + J_{SURF}^0, \quad J_\lambda^{MS} = J_{ATM}^{MS} + J_{SURF}^{MS},$$

$$J_{SURF}^0 = B_\lambda\,[T_S(x_0, y_0)]\,\exp(-\tau(\theta)),$$

$$J_{SURF}^{MS} = \int\int_S h_\lambda(x, y, \theta, \tau_{SC}\,B_\lambda)\,[T_S(x, y)]\,dx\,dy.$$

Here $J_{ATM}^0$, $J_{SURF}^0$, $J_{ATM}^{MS}$, and $J_{SURF}^{MS}$, are the atmospheric and underlying surface contributions to the intensity of unscattered and scattered radiation, respectively; $(x_0, y_0)$ are the coordinates of the point of sensing; $\theta$ is the zenith angle of observation; $\tau$ is the optical thickness of the atmospheric extinction; $\tau_{SC}$ is that of the aerosol scattering; $B_\lambda$ is Plank's function; $B_\lambda^{-1}$ is inverse Plank's function; $T_S$ is the underlying surface temperature; $h_\lambda(r, \varphi, \theta, \tau_{SC})$ is the point spread function; and, $S$ is the effective domain in which the adjacency effect is formed.[2]

The point spread function was calculated using a modification of local-estimate method on conjugate trajectories.[4] For convenience, we calculated this function in coordinates $(r, \varphi)$, where $r$ is the distance along the Earth's surface from the point of sensing to an arbitrary point $(x, y)$, and $\varphi$ is the azimuth angle.

0235-6880/95/09 756-07 $02.00 

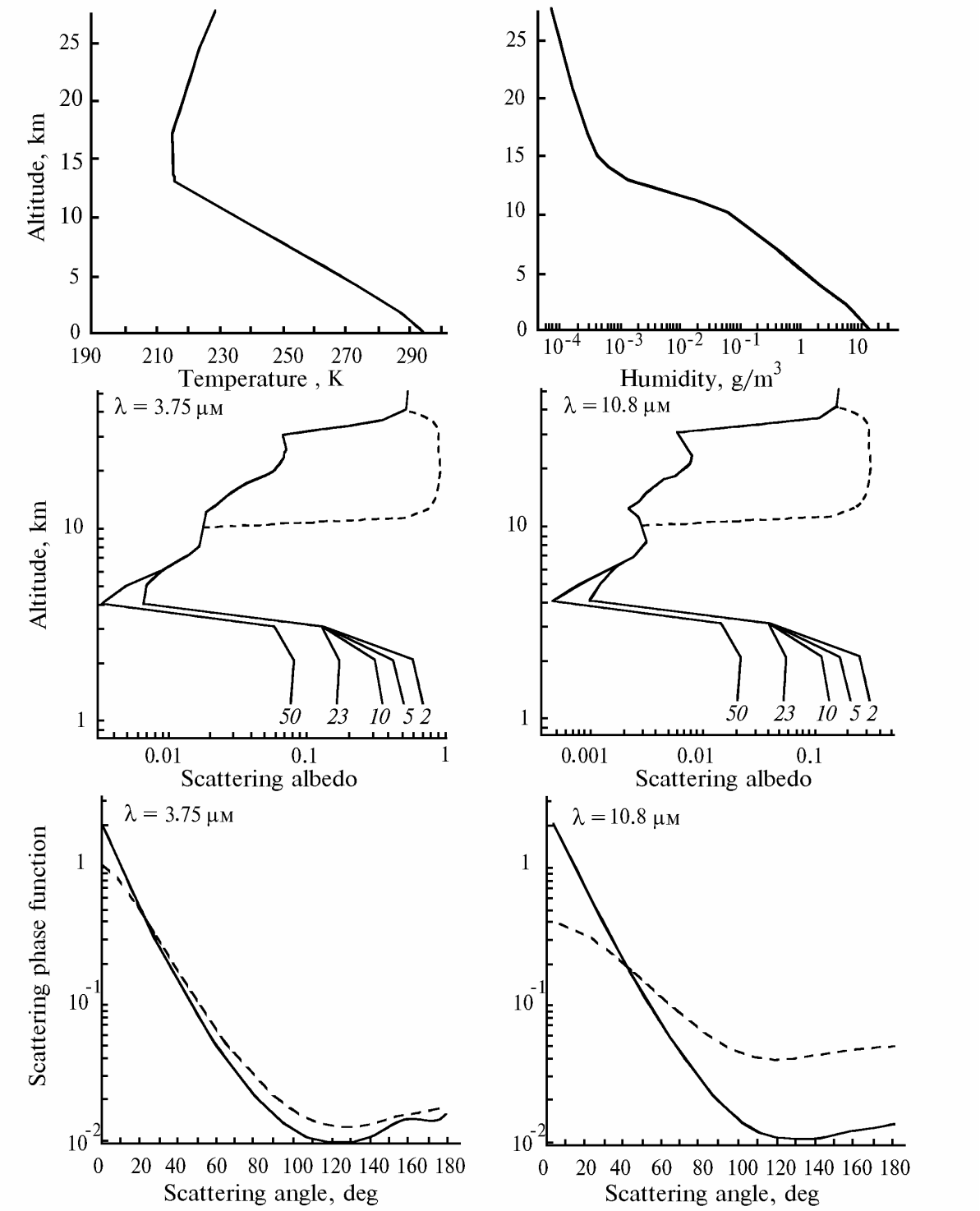


*FIG. 1. Vertical temperature and humidity profiles for the mid-latitude in summer. Vertical profiles of the single scattering albedo for different visibility ranges (2–50 km) in the ground layer for background (solid curves) and postvolcanic (dashed curves) aerosol content in the stratosphere. Angular dependence of the scattering phase function for near-ground (solid curves) and stratospheric (dashed curves) aerosols.*

To calculate $J_{ATM}^{MS}$ as in Refs. 1–3, we used an algorithm for direct simulation on conjugate trajectories.[4] Error in determining the radiative temperature was less than 0.05°.

The range of variation of distances $r$ for simulation by the local-estimate method was chosen to optimize the volume of cumbersome calculations and to provide the algorithmic stability for small values of $r$, as well as on the basis of calculations of the adjacency effect.[2,3] As a result, the range of variations of the values $r$ was 0.01–10 km in the case of near-ground aerosol and 0.1–100 km in the case of postvolcanic one. To calculate the PSF for $r < r_{min}$, we used the method of direct simulation of $J_{\lambda}^{MS}$.

In addition to $h_{\lambda}(r, \varphi, \theta, \tau_{SC})$ the function

$$h_{\lambda}^{*}(\varphi, \theta, \tau_{SC}) = \int_{0}^{R_{max}} h_{\lambda}(r, \varphi, \theta, \tau_{SC})\, r\, dr$$

(integral PSF) was calculated, where $R_{max}$ is the radius of the adjacency effect for the given accuracy of simulation of radiative temperature.

## 3. OPTICAL AND GEOMETRIC CONDITIONS OF SIMULATION

In Refs. 1–3 we considered a wide variety of the optical-meteorological atmospheric parameters. Results presented in that papers allow us to use a meteorological model of the atmosphere (for mid-latitudes in summer) to study the PSF dependence on optical-geometric parameters $(r, \varphi, \theta, \tau_{SC})$, because it is precisely this model for which considerable temperature inhomogeneities are often encountered. Aerosol models were chosen to provide a wide range of variation of $\tau_{SC}$.

Simulation was carried out under the following optical and geometric observational conditions: spectral ranges 3.55–3.95 μm ($\lambda$ = 3.75 μm) and 10.33–11.3 μm ($\lambda$ = 10.8 μm); angles of observation $\theta$ = 0, 30, 45, and 55°; altitude of observation was 800 km; the atmosphere was assumed cloudless, molecular-aerosol, spherically symmetric, and vertically stratified; meteorological model of the atmosphere was used for the mid-latitudes in summer; and, aerosol models were used for maritime aerosol in the ground atmospheric layer 0–2 km (for visibility range $S_M$= 2–50 km) and background aerosol content in the troposphere and the stratosphere. In postvolcanic situation, we used the fresh volcanic aerosol extinction model with moderate, high, and extreme aerosol content in the stratosphere, while the ground layer was assumed free of aerosol. The vertical profiles of meteorological parameters of the atmosphere, the coefficients of molecular and aerosol extinction (scattering), the single scattering albedo, and the scattering phase functions were borrowed from the computer code[5] LOWTRAN-7. Figure 1 shows the optical–meteorological models of the atmosphere used in calculations.

## 4. SIMULATION RESULTS

Let us analyze the behavior of the point spread function $h_{\lambda}(r, \varphi, \theta, \tau_{SC})$ as a function of the distance $r$, azimuth angle $\varphi$, zenith angle of observation $\theta$, and optical thickness of aerosol scattering $\tau_{SC}$. Calculated data are shown in Figs. 2–4. For more vivid presentation, the PSF calculated for near-ground aerosol are shown in Fig. 2 only for $r < 1$ km, i.e., for the domain that makes predominant contribution to the intensity of the adjacency effect.[2]

### 4.1. Near-ground aerosol

The function $h(r)$ decreases monotonically and fast as $r$ increases in the range $r$ | 0.01–10 km considered in this case (Fig. 2). The value of $\partial h(r)/\partial r$ depends on $\tau_{SC}$, $\theta$, and $\varphi$. In particular, $|\partial h(r)/\partial r|$ decreases with increasing $\theta$.

The PSF dependence on the azimuth angle $h(\varphi)$ for near-ground aerosol (Fig. 2) has the following characteristic features for $r < 1$ km:

– occurrence of the maximum at angles $\varphi = \varphi_{min}$ | 60–75°;

– occurrence of the weak maximum at $\varphi$ | 10–20°;

– insignificant variations of the function in the range $\varphi = 0° - \varphi_{min}$;

– significant (several times) increase of $h(\varphi)$ with increase of $\varphi$ for $\varphi > \varphi_{min}$;

– increase of $|\partial h(\varphi)/\partial \varphi|$ with increasing $\theta$.

In addition, one more feature should be noted in the behavior of $h(\varphi)$ for $r < 1$ km: the point of the minimum is displaced toward $\varphi_{min}$ | 90–120°. The amount of this displacement increases with increasing optical thickness and decreasing zenith angle of observation.

The features are vividly seen from the azimuth dependence of the integral PSF $h^{*}(\varphi)$, normalized by unity, shown in Fig. 4. Comparison of the data shown in Fig. 4 with the dependence of the scattering phase function on the scattering angle $P(\varphi^{*})$ shown in Fig. 1 indicates a similarity of their behavior for contiguous angles $\varphi$ and $180° - \varphi^{*}$. In addition, high correlation between their angular behavior and values of the function $h^{*}(\varphi)$ under conditions of high and low transmission of the atmosphere should be noted.

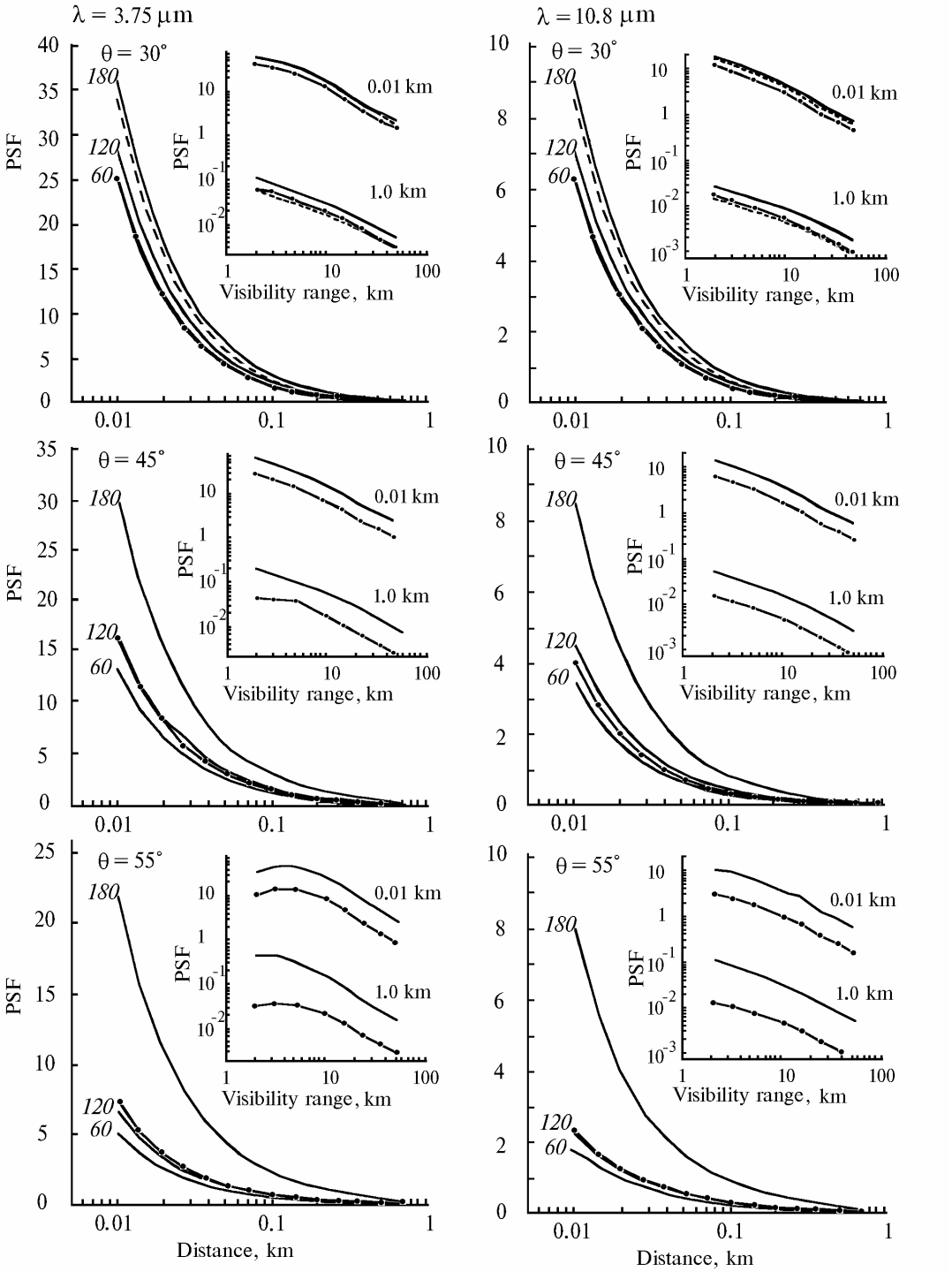


*FIG. 2. Point spread function $h(r, \varphi)$ in the case of near-ground aerosol ($S_M$ = 5 km) at azimuth angles of observation* $\varphi$ = 0, 60, 120, *and* 180° *and zenith angles of observation* $\theta$ = 30, 45, *and* 55°. *Incorporated figures: dependence of* $h(r, \varphi)$ *on the visibility range for* $r$ = 0.01 *and* 1.0 km *and* $\varphi$ = 0 *and* 180°. *Solid curves with dots are for* $\varphi$ = 0° *and dashed curves are for* $\theta$ = 0°.

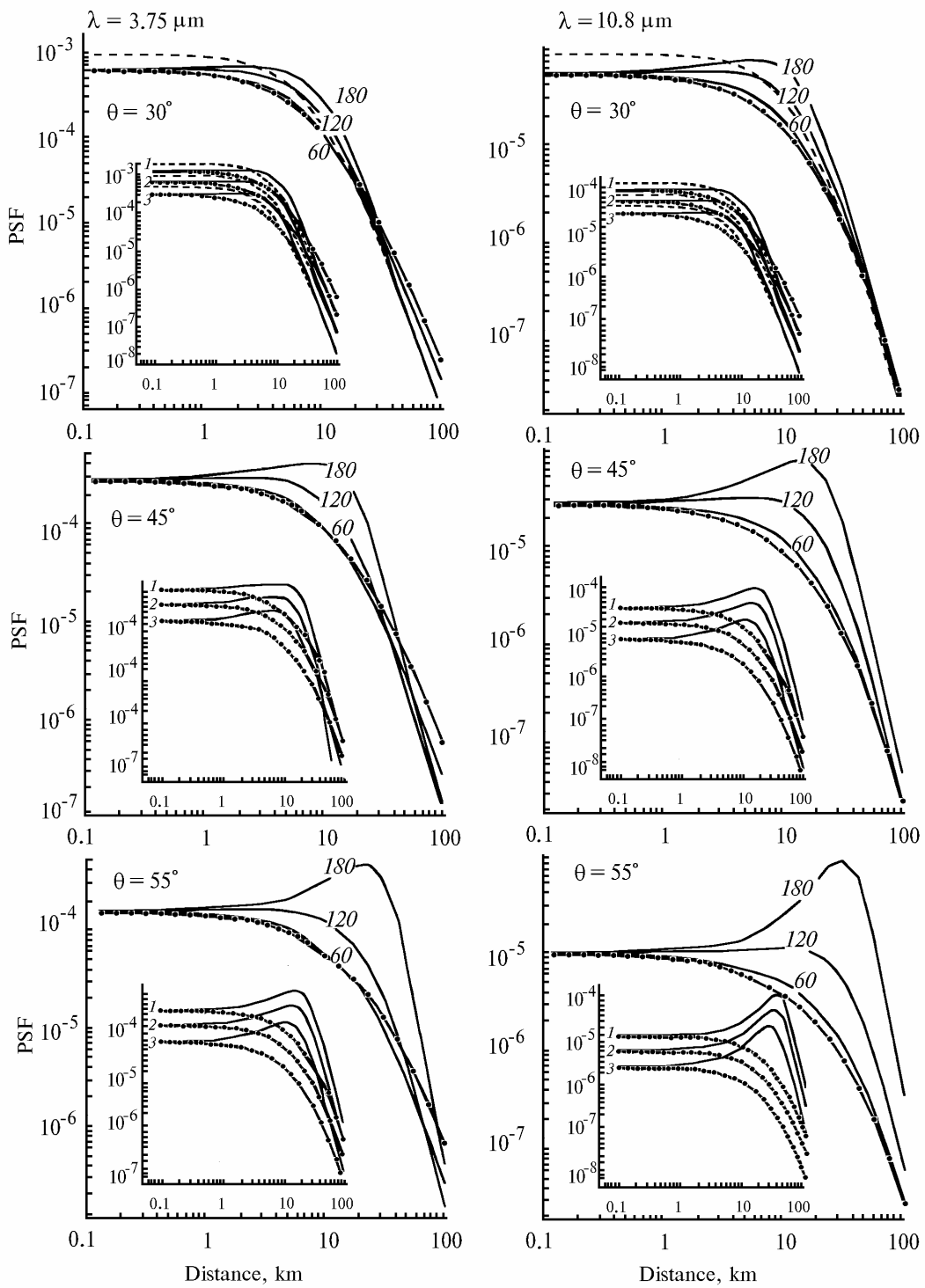


*FIG. 3. Point spread function h(r, φ) in the case of high content of postvolcanic stratospheric aerosol at azimuth angles* φ = 0, 60, 120, *and* 180° *and zenith angles of observation* θ = 30, 45, *and* 55°. *Incorporated figures: the function h(r,* φ*) for extreme (1), high (2), and moderate (3) content of postvolcanic aerosol in the stratosphere at* φ = 0 *and* 180°. *Solid curves with dots are for* φ = 0°, *and dashed curves are for* θ = 0°.

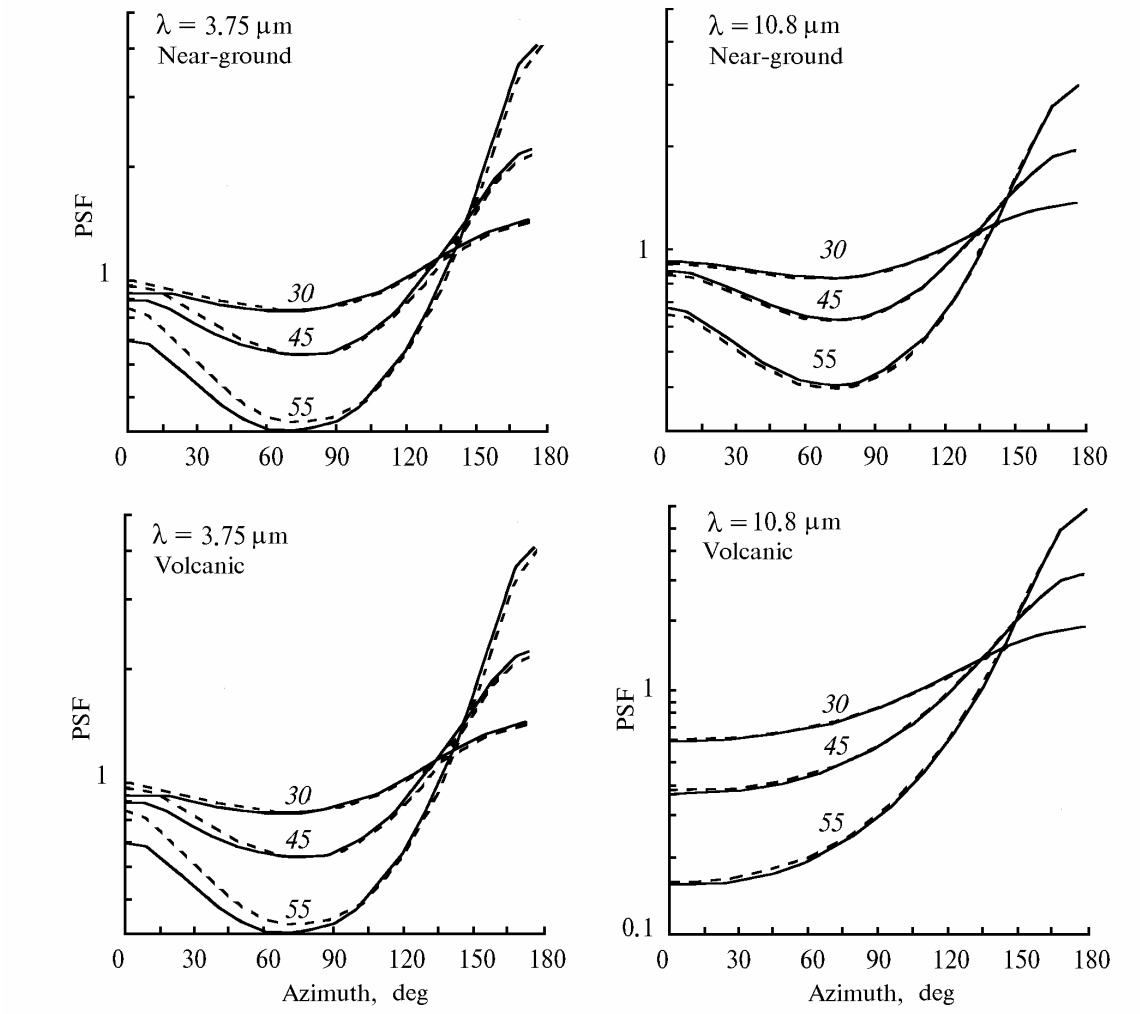


*FIG. 4. The function $h^*(r, \varphi)$ for near-ground and stratospheric aerosols at different zenith angles of observations* $\theta = 30$, 45, *and* 55°. *Near-ground aerosol:* $S_M = 5$ *and* 23 km *(solid and dashed curves, respectively). Stratospheric aerosol: extreme (solid curves) and moderate (dashed curves) content.*

The PSF dependence on the zenith angle of observation $h(\theta)$ has two characteristic features: $\partial h(\theta)/\partial\theta < 0$ for $r < r_1$, and $\partial h(\theta)/\partial\theta > 0$ for $r > r_2$. Values of $r_1$ and $r_2$ vary under different optical-geometric conditions of observation. The dependence of $r_1$ and $r_2$ on the azimuth angle is most clearly pronounced. It is characterized by the maximum values of the pairs $r_1$ and $r_2$ at $\varphi = \varphi_{min}$ and their minimum values at $\varphi = 180$. On the whole, $r_1$ is less than 1–5 km (for different values of $\varphi$ and $\tau_{SC}$), and $r_2$ is greater than 0.2–1 km.

The PSF dependence on visibility range $S_M$ has the following characteristic features: the function $h(S_M)$ decreases monotonically with increasing $S_M$, the tendency to disturbance in monotonicity of the function $h(S_M)$ becomes more pronounced for $\lambda = 3.75$ μm with increasing zenith angle of observation for low visibility ranges $S_M < 5$ km.

These salient features of the dependence $h(S_M)$ are vividly illustrated by the plots incorporated in Fig. 2. In Ref. 2 we obtained analogous dependence for the function $F(r)$ and put forward the explanation of such behavior for low values of $S_M$.

### 4.2. Postvolcanic aerosol

In this case the dependence $h(r)$ is described by monotonically decreasing function with increasing $r$ within the considered range of distances $r \mid 0.1–10$ km at $\varphi < 100–200°$ (see Fig. 3).

However, when φ increases at θ > 0°, the function $h(r)$ has the clearly pronounced maximum, whose position ($r_{max}$) and altitude ($h_{max}$) depend on φ, θ, and $\tau_{SC}$. In particular, increase of $r_{max}$ then reaches values of the order of 15–30 km at φ = 180 and θ = 55°. These salient features are most vividly illustrated by the graphs incorporated in Fig. 3.

The azimuth dependence of PSF has the following salient features: $\partial h(\theta)/\partial\theta > 0$ for $r < r^*$; $|\partial h(\theta)/\partial\theta|$ increases with increasing θ. Values of $r^*$ are within the range $r$ = 5–10 km for λ = 3.75 μm, and $r$ = 30–70 km for λ = 10.8 μm.

In Fig. 4, the azimuth dependence of the integral PSF is shown for aerosol of this type. Comparing the behavior of the function $h^*(\varphi)$ and the angular dependence of the scattering phase function, we can notice, as previously, their similarity. One also can note the identity of the angular dependence and fair coincidence of the values of $h^*(\varphi)$ for different $\tau_{SC}$.

The PSF dependence on zenith angle of observation has the same characteristic features as in the case of near-ground aerosol: $\partial h(\theta)/\partial\theta < 0$ for $r < r_1$, and $\partial h(\theta)/\partial\theta > 0$ for $r > r_2$. However, in contrast to the case of near-ground aerosol, the value of $r_2$ decreases monotonically with increasing azimuth angle. Ranges of variations of $r_1$ are 5–20 km (λ = 3.75 μm) and 5–60 km (λ = 10.8 μm), and the values of $r_2$ exceed 15–30 km.

The PSF dependence on optical thickness is illustrated by the graphs incorporated in Fig. 3 that demonstrate the increase of the PSF values with increasing $\tau_{SC}$ in the entire ranges of variations of θ and φ.

## 5. CONCLUSION

Generalizing the regularities in the PSF behavior as a function of the optical-geometric parameters $r$, φ, θ, and $\tau_{SC}$, it should be noted that the PSF has ambiguous character complicated for construction of suitable approximations. Nevertheless, based on the characteristics of the function $h^*(\varphi)$ and the extent to which the variations in the optical-meteorological parameters affect the characteristics of the adjacency effect,[1–3] we can draw the following important practical conclusion. For a rather wide range of variability of the meteorological parameters of the atmosphere and the optical parameters of aerosol scattering, it is acceptable to use a universal data set to correct for the atmospheric contribution at given values of φ and θ under different conditions of atmospheric turbidity.

To estimate the validity of this conclusion, we plan to perform additional study on the basis of imitation simulation. However, we have already obtained preliminary data in the simple case, in which the domain of existence of the adjacency effect may be subdivided into two subdomains with different temperature $T_1$ and $T_2$. In this case the use of PSF for maximum turbidity of the atmosphere results in an error in calculating no more than 0.5° even in the case of lower values of $\tau_{SC}$ in which the temperature gradient is of the order of 20° (near-ground aerosol, φ = 180°, θ = 55°, and λ = 3.75 μm). This result is in good agreement with our conclusion.

## REFERENCES

1. S.V. Afonin, V.V. Belov, and I.Yu. Makushkina, Atmos. Oceanic Opt. **7**, No. 6, 423–429 (1994).
2. S.V. Afonin, V.V. Belov, and I.Yu. Makushkina, Atmos. Oceanic Opt. **7**, No. 6, 430–434 (1994).
3. S.V. Afonin, V.V. Belov, and I.Yu. Makushkina, Atmos. Oceanic Opt. **7**, No. 6, 435–440 (1994).
4. V.V. Belov, and I.Yu. Makushkina, in: *Theory and Applications of Statistical Simulation* (Computer Center of the Siberian Branch of the Academy of Sciences of the USSR, Novosibirsk, 1988), pp. 153–164.
5. F.X. Kneizys, et al., "*User's guide to LOWTRAN-7*," Report AFGL-TR-88-0177 ERP, No. 1010 (Hansom, 1988).